International Journal of Multidisciplinary Science and Innovation (IJMSI)
International Conference on Advances in Physical, Chemical and Mathematical Sciences for Sustainable Development
Organized by
D.M.S. Mandal's Bhaurao Kakatkar College, Belgaum, Karnataka, India
Website: https://ijmsi.in/
ISSN: 3107-5754 I Vol. 2, Special Issue 1, 2026 I Page No.: 139-151

Research

Analysis of MHD Squeezing Flow and Radiative Heat Transfer of Ethylene Glycol-Based Magnetite Nanofluid Between Parallel Disks by Chebyshev Pseudo-Spectral Method

Yashodha S. Sindhe[1*], Vishwanath B. Awati[2], Mahesh Kumar N.[3]
[1]*School of Commerce and Management, Sri Balaji University, Pune*
[2.3]*Department of Mathematics, Rani Channamma University, Belagavi 591156, India*

Corresponding Author:
Yashodha S. Sindhe

Email: *ysindhe@gmail.com*

DOI: *10.62896/ijmsi.2.s1.17*

Conflict of interest: *NIL*

Article History
Received: 08/06/2026
Accepted: 16/06/2026
Published: 20/06/2026

Abstract:
This study presents a theoretical investigation of the magnetohydrodynamic (MHD) flow and heat transfer characteristics of an ethylene glycol ($C_2H_6O_4$)-based nanofluid containing magnetite (Fe_3O_4) nanoparticles confined between two parallel disks undergoing squeezing motion, incorporating the effects of an applied magnetic field and thermal radiation. The governing nonlinear partial differential equations are transformed into a system of nonlinear ordinary differential equations using appropriate similarity transformations. The resulting boundary value problem is then evaluated. numerically using the Chebyshev Pseudo-Spectral Method (CPSM) to obtain highly accurate solutions. The analysis focuses on the velocity and temperature distributions, skin friction coefficient, and Nusselt number for various physical parameters such as magnetic field strength, nanoparticle volume fraction, radiation parameter, and squeezing effect. The results demonstrate that the applied magnetic field significantly influences the flow behavior, while increasing the concentration of magnetite nanoparticles enhances the heat transfer rate and surface skin friction. These findings confirm the potential of magnetite-enhanced ethylene glycol nanofluids for improved thermal performance in advanced heat transfer systems.

Keywords: Ethylene glycol nanofluid; Magnetite nanoparticles; MHD squeezing flow; Thermal radiation; Parallel disks; Chebyshev Pseudo-Spectral Method; Skin friction; Nusselt number.

1. Introduction:

The study of fluid flow and heat transfer between parallel disks has long attracted attention due to its applications in lubrication systems, polymer processing, hydraulic brakes, and cooling of rotating machinery. One of the earliest investigations was conducted by S. Ishizawa, analyzed unsteady flow between parallel disks and highlighted the influence of squeezing motion on velocity distribution [6]. Later, G. L. Mellor and co-workers extended the analysis to rotating disk configurations and reported multiple solution branches for viscous incompressible flow [7]. Further improvements were made by U. Nazir and T. Mahmood, incorporated heat transfer effects into the rotating disk problem, providing insight into temperature variations in confined geometries [8].

The introduction of nanofluids significantly enhanced the thermal performance of conventional heat transfer fluids. The concept of nanofluids was

International Journal of Multidisciplinary Science and Innovation (IJMSI)
International Conference on Advances in Physical, Chemical and Mathematical Sciences for Sustainable Development
Organized by
D.M.S. Mandal's Bhaurao Kakatkar College, Belgaum, Karnataka, India
Website: https://ijmsi.in/
ISSN: 3107-5754 I Vol. 2, Special Issue 1, 2026 I Page No.: 139-151

first proposed by S. U. S. Choi [1], demonstrated that dispersing nanoparticles into base fluids can enhance thermal conductivity. Subsequently, experimental studies by J. A. Eastman and co-authors [2] reported remarkable increases in thermal conductivity for ethylene glycol-based nanofluids. Theoretical and experimental contributions by Y. Xuan and Q. Li [3], and S. K. Das et al. [4] further demonstrated that nanoparticle concentration and temperature strongly influence heat transfer enhancement. A comprehensive theoretical model explaining convective transport in nanofluids was later proposed by J. Buongiorno [5], identified Brownian motion and thermophoresis as dominant mechanisms.

In recent years, attention has shifted toward magnetohydrodynamic (MHD) squeezing flow of nanofluids due to its importance in metallurgical processing, cooling of electronic devices, and magnetic drug targeting. Studies such as those by Hayat et al. [9] examined irreversibility effects in squeezing nanofluid flows with thermal radiation. Zainal et al. [10] investigated MHD and radiation effects in hybrid nanofluids, while Hosseinzadeh et al. [11] analyzed entropy generation in magnetite-based nanofluids under nonlinear radiation. More recently, Awati et al. [12] applied spectral and Haar wavelet collocation techniques to analyze heat generation and viscous dissipation in micro-polar nanofluid stagnation point flow. Awati et al. [13] further studied stability characteristics of Casson fluid flow using spectral methods. Additional developments include Maxwell nanofluid squeezing flows [14], hybrid nanofluid thermal behavior [15], and irreversibility analysis between permeable disks [16]. Recent investigations by Vigneshwari et al. [17] and Johari et al. [18] emphasized the importance of magnetic field and generalized heat flux models in controlling temperature distribution. These studies demonstrate that the combined effects of magnetic field, radiation, and nanoparticle properties significantly influence thermal transport.

Spectral and pseudospectral techniques have become powerful tools for solving nonlinear boundary value problems arising in fluid mechanics. One of the earliest applications of Chebyshev spectral collocation for viscous flows was reported by Farcy and de Roquefort [20], analysed incompressible Navier–Stokes equations in curvilinear domains. Guo and Li [21] extended Fourier–Chebyshev pseudospectral schemes to two-dimensional vorticity equations. Later, Elazem and Ebaid [22] demonstrated the robustness of Chebyshev pseudospectral methods for nonlinear boundary value problems, while Elgazery [23] applied implicit Chebyshev discretization to study radiation effects in non-Newtonian fluids. Recent advancements include applications to fractional differential equations by Oloniiju et al. [24,28] and further developments in optimal control using pseudospectral approaches by Elnagar et al. [26] and Fahroo and Ross [27]. Yousefian et al. [29] introduced a novel online pseudospectral framework for nonlinear dynamical systems. These studies confirm that the Chebyshev pseudospectral method provides exponential convergence, high accuracy, and computational efficiency. Therefore, the present work employs this method to analyze MHD squeezing flow and radiative heat transfer of ethylene glycol-based magnetite nanofluid between parallel disks.

2. Mathematical formulation

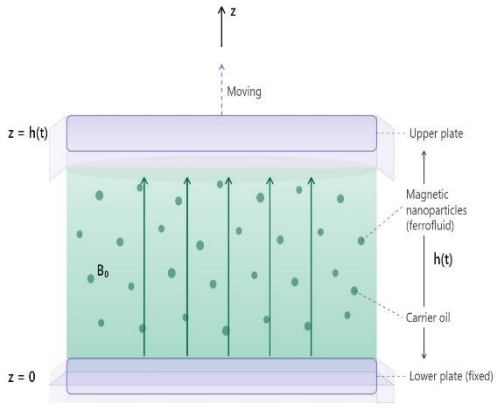

Fig. 1 Geometry of the flow

Consider the incompressible magneto hydrodynamic (MHD) flow of an ethylene glycol–based nanofluid containing magnetite nanoparticles, confined between two infinite parallel disks separated by a finite distance $h(t)$. Let $B_0(1-at)^{\left(-\frac{1}{2}\right)}$ be the applied magnetic field normal to the disks. Let T_0 and T_1 be the temperatures of the bottom and top disks,

Website: https://ijmsi.in/
ISSN: 3107-5754 I Vol. 2, Special Issue 1, 2026 I Page No.: 139-151

respectively. In the considered problem, it is assumed that the upper disk moves towards and away from the fixed lower disk at a velocity $\frac{aH(1-at)^{\left(=\frac{1}{2}\right)}}{2}$ as shown in Fig. 1. , as reported by Sampath Kumar et. al[23].

The equations governing flow and energy of an unsteady incompressible flow of a viscous fluid in three dimensional cylindrical coordinates are thus given by, $\frac{1}{R}\frac{\partial(Ru)}{\partial R}+\frac{1}{R}\frac{\partial v}{\partial\theta}+\frac{\partial w}{\partial z}=0$ (1)

$$\rho\left(\frac{\partial u}{\partial t}+u\frac{\partial u}{\partial R}+\frac{v}{R}\frac{\partial u}{\partial\theta}-\frac{v^2}{R}+w\frac{\partial u}{\partial z}\right)=-\frac{\partial p}{\partial R}+\mu\left(\nabla^2u-\frac{u}{R^2}-\frac{2}{R^2}\frac{\partial v}{\partial\theta}\right)-\sigma B^2(t)u, \quad (2)$$

$$\rho\left(\frac{\partial v}{\partial t}+u\frac{\partial v}{\partial R}+\frac{v}{R}\frac{\partial v}{\partial\theta}+\frac{uv}{R}+w\frac{\partial v}{\partial z}\right)=-\frac{1}{R}\frac{\partial p}{\partial\theta}+\mu\left(\nabla^2v-\frac{v}{R^2}-\frac{2}{R^2}\frac{\partial u}{\partial\theta}\right), \quad (3)$$

$$\rho\left(\frac{\partial w}{\partial t}+u\frac{\partial w}{\partial R}+\frac{v}{R}\frac{\partial w}{\partial\theta}+w\frac{\partial w}{\partial z}\right)=-\frac{\partial p}{\partial z}+\mu\nabla^2w, \quad (4)$$

$$\begin{aligned}\rho C_p\left(\frac{\partial T}{\partial t}+u\frac{\partial T}{\partial R}+\frac{v}{R}\frac{\partial T}{\partial\theta}+\frac{uv}{R}+w\frac{\partial T}{\partial z}\right)&\\ =k\nabla^2T+2\mu\left(\frac{\partial u}{\partial R}\right)^2+2\mu\left[\frac{1}{R}\left(\frac{\partial v}{\partial\theta}+u\right)\right]^2&\\ +2\mu\left(\frac{\partial w}{\partial z}\right)^2&\\ +\mu\left[\left(\frac{\partial v}{\partial z}+\frac{1}{R}\frac{\partial w}{\partial\theta}\right)^2+\left(\frac{\partial w}{\partial R}+\frac{\partial u}{\partial z}\right)^2+\left(\frac{1}{R}\frac{\partial u}{\partial\theta}+R\frac{\partial\left(\frac{v}{R}\right)}{\partial R}\right)^2\right]&\end{aligned} \quad (5)$$

Where $\nabla^2=\frac{1}{R}\frac{\partial}{\partial R}\left(R\frac{\partial}{\partial R}\right)+\frac{1}{R^2}\frac{\partial^2}{\partial\theta^2}+\frac{\partial^2}{\partial z^2}$.

In the above set of equations, $\frac{\partial p}{\partial z}=0$, as there exists rotational symmetry in the flow. Further, the azimuthal element of the velocity $V=(u,v,w)$ disappears, that is, $v=0$. Here, the velocity components of the flow along R−axis, θ −axis, and z−axis are denoted by u, v, and w, respectively, and the pressure is denoted by p. The specific heat capacity, dynamic viscosity, thermal conductivity, and density of the fluid are respectively represented by C_p , μ, k and ρ . Thus, the two dimensional viscous incompressible flow of the MHD nanofluids is governed by,

$$\frac{\partial u}{\partial R}+\frac{u}{R}+\frac{\partial w}{\partial z}=0, \quad (6)$$

$$\rho_{nf}\left(\frac{\partial u}{\partial t}+u\frac{\partial u}{\partial R}+w\frac{\partial u}{\partial z}\right)=$$
$$-\frac{\partial p}{\partial R}+\mu_{nf}\left(\frac{\partial^2 u}{\partial R^2}+\frac{1}{R}\frac{\partial u}{\partial R}-\frac{u}{R^2}+\frac{\partial^2 u}{\partial z^2}\right)-\sigma B^2(t)u, \quad (7)$$

$$\rho_{nf}\left(\frac{\partial w}{\partial t}+u\frac{\partial w}{\partial R}+w\frac{\partial w}{\partial z}\right)=-\frac{\partial p}{\partial z}+\mu_{nf}\left(\frac{\partial^2 w}{\partial R^2}+\frac{1}{R}\frac{\partial w}{\partial R}+\frac{\partial^2 w}{\partial z^2}\right), \quad (8)$$

$$\left(\rho C_p\right)_{nf}\left(\frac{\partial T}{\partial t}+u\frac{\partial T}{\partial R}+w\frac{\partial T}{\partial z}\right)=k_{nf}\left(\frac{\partial^2 T}{\partial R^2}+\frac{1}{R}\frac{\partial T}{\partial R}+\frac{\partial^2 T}{\partial z^2}\right)-\frac{\partial q_r}{\partial z}, \quad (9)$$

Where $\mu_{nf}, \rho_{nf}, k_{nf}$, $C_{p_{nf}}$ and q_r denote the dynamic viscosity, density, thermal conductivity, specific heat capacity of the nanpfluid and radiative heat flux respectively. Further,

$$\mu_{nf}=\frac{\mu_f}{(1-\phi)^{2.5}}, \alpha_{nf}=\frac{k_{nf}}{(\rho C_p)_{nf}}, \frac{k_{nf}}{k_f}=\frac{(2k_f+k_s)-2\phi(k_f-k_s)}{(2k_f+k_s)+\phi(k_f-k_s)},$$

$$\rho_{nf}=(1-\phi)\rho_f+\phi\rho_s, \nu_{nf}=\frac{\mu_{nf}}{\rho_{nf}}, (\rho C_p)_{nf}=(1-\phi)(\rho C_p)_f+\phi(\rho C_p)_s, q_r=-\frac{4\sigma^*}{3k^*}\frac{\partial T^4}{\partial z}$$

Here, the specific heat capacity, dynamic viscosity, thermal conductivity, and density of the base fluid are respectively represented by C_{p_i}, μ_f, k_f and ρ_f. The nanoparticle's solid volume fraction is given by ϕ, and C_{p_s}, ρ_s and k_s respectively denote the specific heat capacity, density and thermal con ductivity of the solid fraction. α_{nf} and ν_{nf} denote the thermal diffusivity and kinematic viscosity of the nanofluid. The boundary conditions to the considered problem are given by,

$$u=0, w=\frac{dh}{dt}, T=T_1 \ \ at \ z=h(t), u=0, \ \ w=0, \ \ T=T_0, \ \ at \ \ z\to 0.$$

For an optically thick fluid, assuming small temperature differences within the flow, T^4 can be expanded using a Taylor series about T_h: $T^4 \approx 4T_h{}^3T-3T_h{}^4$ This linearization leads to: $\frac{\partial q_r}{\partial z}=-\frac{16\sigma^* T_h{}^3}{3k^*}\frac{\partial^2 T}{\partial z^2}$

The nonlinear PDEs that govern the flow and energy are transformed into nonlinear ODEs by employing the similar ity transformations as follows:

$$B(t)=\frac{B_0}{(1-at)^{\frac{1}{2}}}, \quad (10)$$

$$\eta=\frac{z}{H(1-at)^{\frac{1}{2}}}, \quad (11)$$

$$u=\frac{ar}{(1-ar)}F'(\eta) \quad (12)$$

$$w=\frac{aH}{(1-at)^{\frac{1}{2}}}f(\eta), \quad (13)$$

$$\theta = \frac{T - T_1}{T_2 - T_1}, \tag{14}$$

Adopting the transformations Eqs. (10–14) in Eqs. (7–9) and eliminating the pressure gradient, the following equations are obtained,

$$\frac{1}{(1-\phi)^{2.5}} F^{iv}(\eta) + S\left[(1-\phi) + \phi\frac{\rho_s}{\rho_f}\right]\left[F'''(\eta)F(\eta) - 3F''(\eta) - \eta F'''(\eta)\right] - MF''(\eta) = 0, \tag{15}$$

$$\left(\frac{k_{nf}}{k_f} + Rd\right)\theta''(\eta) + S\,\mathrm{Pr}\left((1-\phi) + \phi\frac{(\rho C_p)_s}{(\rho C_p)_f}\right)\left(2F(\eta)\theta'(\eta) - \eta\theta'(\eta)\right) = 0, \tag{16}$$

along with the boundary conditions,

$$F(0) = 0,\ F(1) = \frac{1}{2}, F'(0) = 0, F'(1) = 0, \theta(0) = 1, \theta(1) = 0. \tag{17}$$

Correspondingly the squeeze number, magnetic parameter, and Prandtl number are respectively defined as follows,

$$C_f = \frac{\mu_{nf}\left(\frac{\partial u}{\partial z} + \frac{\partial w}{\partial R}\right)_{z=h(t)}}{\rho_{nf}\left(\frac{-aH}{2\sqrt{1-at}}\right)^2},\quad Nu = \frac{k_{nf}\left(\frac{\partial T}{\partial z}\right)_{z=h(t)}}{k_f\left(T_w - T_h\right)}. \tag{19}$$

Substituting Eqs. (10–14) in Eq. (19),

$$\frac{H^2}{R^2}\,\mathrm{Re}\,C_f = \frac{1}{\left((1-\phi) + \phi\frac{\rho_s}{\rho_f}\right)}F''(1), \qquad (1-at)^{\frac{1}{2}}\,Nu = -\left(\frac{k_{nf}}{k_f} + Rd\right)\theta'(0). \tag{20}$$

Here, local Reynolds number Re is defined as,

$$\mathrm{Re} = \frac{\rho_f raH(1-at)^{\frac{1}{2}}}{a\mu_f}.$$

Radiation parameter $Rd = \dfrac{16\sigma^* T_h^{\,3}}{3k_f k^*}$

3. Method of solution

The transformed nonlinear ordinary differential equation governing the steady magnetohydrodynamic Casson fluid flow in a porous channel is numerically analyzed using the Chebyshev pseudospectral method, and the corresponding algorithm is implemented in Mathematica. The nonlinear system is linearized using an approach inspired by the Newton–Raphson method, which ensures efficient iterative convergence.

The Chebyshev pseudospectral method, originally introduced by Elnagar et al. [24] and later refined by Fahroo and Ross [25], has been extensively utilized in optimal control problems and fractional differential equations due to its high accuracy and rapid convergence for smooth solutions over finite domains. Furthermore, Shina Daniel Oloniiju et al. [26] successfully applied this method to fractional differential equations in partitioned domains. Similarly, Arian Yousefian et al. [27], along with Narayanan, developed an online pseudospectral framework based on Chebyshev polynomial bases for system identification under aperiodic sampling conditions. Chebyshev polynomials (T_k) are defined on the interval $\xi \in [-1,1]$.physical channel is defined on $\eta \in [0,1]$We map the physical space to the spectral space using:

$$\xi = 2\lambda - 1$$

This ensures $\lambda = 0$ (lower wall) maps to $\xi = -1$, and $\lambda = 1$ (upper wall) maps to $\xi = 1$.

assume the stream function $f(\lambda)$ can be represented as a sum of $N+1$ Chebyshev polynomials:

$$f(\xi) \approx \sum_{k=0}^{N} a_k T_k(\xi)$$

where a_k are the unknown coefficients to be evaluated..

Collocation at Gauss-Lobatto Nodes clustered near the walls:

$\xi_i = \cos\left(\frac{\pi i}{N}\right)$, $i = 0,1,\ldots,N$, are the Chebyshev–Gauss–Lobatto points.

Derivatives of a function at the collocation points are approximated via matrix multiplication. Let $f = [f(\xi_0), f(\xi_1), \ldots, f(\xi_N)]^T$. The first derivative is

$$\left.\frac{dy}{d\xi}\right|_{\xi=\xi_i} = \sum_{j=0}^{N} D_{ij}\, y(\xi_j), \quad i = 0,\ldots,N,$$

The Chebyshev differentiation matrix, denoted by D, is a square matrix of order $(N+1)\times(N+1)$.

$$D_{ij} = \begin{cases} \dfrac{2N^2+1}{6}, & i = j = 0, \\ -\dfrac{2N^2+1}{6}, & i = j = N \\ -\dfrac{\xi_i}{2(1-\xi_i^2)}, & 1 \le i = j \le N-1, \\ \dfrac{c_i}{c_j}\dfrac{(-1)^{i+j}}{\xi_i - \xi_j}, & i \ne j, \end{cases} \qquad c_0 = c_N = 2, c_i = 1 \ (1 \le i \le N-1).$$

The derivative of the function at all nodes is calculated simultaneously:

$$F' = 2DF,\ F'' = 4D^2F,\ F''' = 8D^3F, F^{iv} = 16D^4F$$

Discretized Governing Equations

Substituting the matrix operators into the governing ODEs results in a system of nonlinear algebraic equations:

Momentum Equation (from Eq. 15):

$$\frac{16}{(1-\phi)^{2.5}} D^4F + S\left[(1-\phi)+\phi\frac{\rho_s}{\rho_f}\right]\left[\left(8D^3F\right)\cdot F - 3\left(4D^2F\right) - \eta\cdot\left(8D^3F\right)\right] - M\left(4D^2F\right) = 0$$

Energy Equation (from Eq. 16):

$$\left(\frac{k_{nf}}{k_f} + Rd\right)\left(4D^2\theta\right) + S\,\mathrm{Pr}\left[(1-\phi)+\phi\frac{(\rho C_p)_s}{(\rho C_p)_f}\right]\left[2F\cdot(2D\theta) - \eta\cdot(2D\theta)\right] = 0$$

Because the resulting system is nonlinear, an iterative solver like the Newton-Raphson method is typically applied. The initial guess used in the study, $F_0(\eta) = \frac{1}{2}\left(3\eta^2 - 2\eta^3\right)$ and $\theta_0(\eta) = 1-\eta$, provides a starting point that satisfies the boundary conditions. The iteration continues until the residual of the equations reaches a specified tolerance (e.g., 10^{-10}), yielding results that align with the high-accuracy tables provided in the paper.

4. Results and discussion

Property	Ethylene Glycol (Base Fluid)	Magnetite (Nanoparticles)
Density (ρ)	1115 kg/m^3	5180$ kg/m^3
Specific Heat (Cp)	2430 $J/kg\cdot K$	670 $J/kg\cdot K$
Thermal Conductivity (k)	0.253 $W/m\cdot K$	9.7 $W/m\cdot K$
Prandtl Number (Pr)	24.4	—

Table 2 Coefficient of skin friction for different values of ϕ , S, and M

ϕ	S	M	HPM[23]	FDM[23]	CPSM
0.1	0.5	0.1	−3.01071	−3.01000	-3.01055
0.2			−3.17983	−3.17889	-3.17968
0.3			−3.64362	−3.64281	-3.64347
0.1		0.3	−3.01774	−3.01662	-3.01757
0.2			−3.18540	−3.18404	-3.18523
0.3			−3.64824	−3.64790	-3.64808
0.1	−0.2	0.2	−2.80982	−2.80873	-2.80987
0.2			−2.97810	−2.97738	-2.97815
0.3			−3.44131	−3.44008	-3.44136
0.1	0		−2.86832	−2.86633	-2.86831
0.2			−3.03663	−3.03557	-3.03662
0.3			−3.49985	−3.49828	-3.49985
0.1	0.2		−2.92674	−2.92532	-2.92667
0.2			−3.09508	−3.09416	-3.09501
0.3			−3.55833	−3.55764	-3.55827

International Journal of Multidisciplinary Science and Innovation (IJMSI)
International Conference on Advances in Physical, Chemical and Mathematical Sciences for Sustainable Development
Organized by
D.M.S. Mandal's Bhaurao Kakatkar College, Belgaum, Karnataka, India
Website: https://ijmsi.in/
ISSN: 3107-5754 I Vol. 2, Special Issue 1, 2026 I Page No.: 139-151

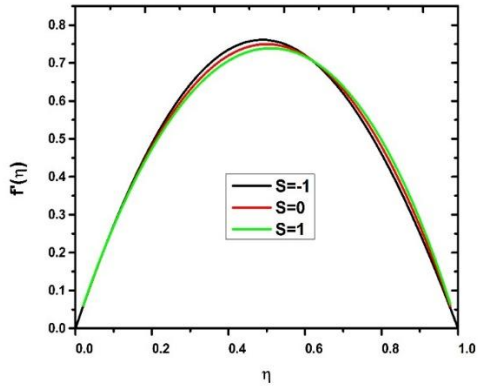

Fig. 2 Velocity profile for different squeeze number when $\phi = 0.1, M = 0.1$

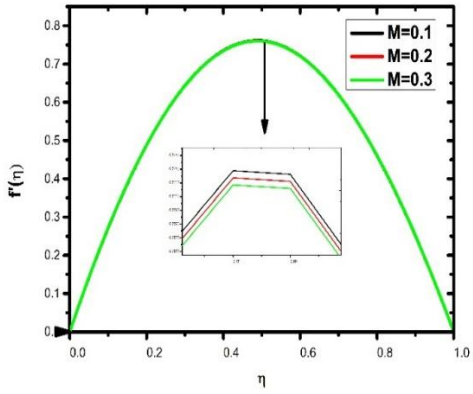

Fig. 5 Velocity profile for different magnetic parameter when $S = -1, \phi = 0.1.$

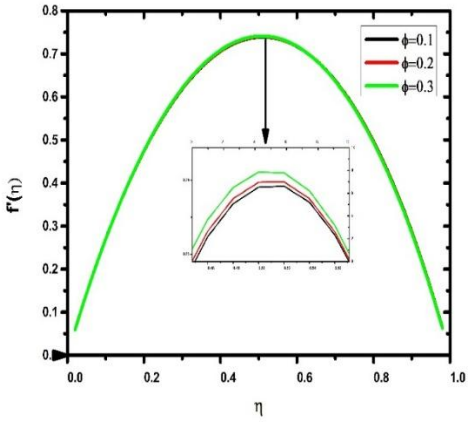

Fig. 3 Velocity profile for different solid volume fraction when $S = -1, M = 0.1.$

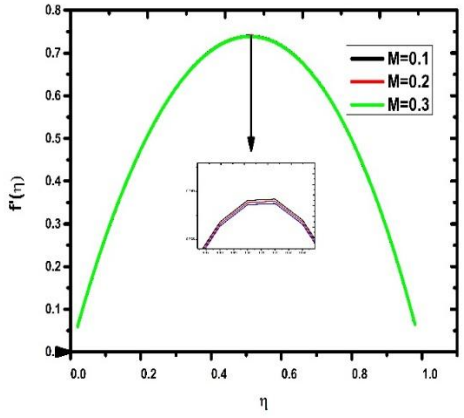

Fig. 6 Velocity profile for different magnetic parameter when $S = 1, \phi = 0.1.$

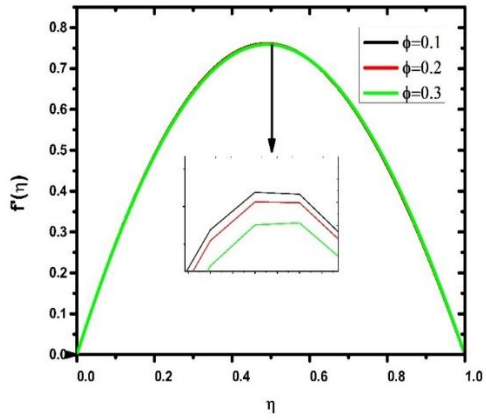

Fig. 4 Velocity profile for different solid volume fraction when $S = 1, M = 0.1.$

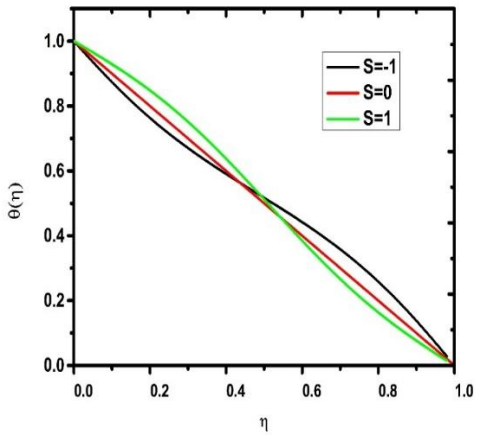

Fig. 7 Temperature profile for different squeeze number when $\phi = 0.1, M = 0.1$

International Journal of Multidisciplinary Science and Innovation (IJMSI)
International Conference on Advances in Physical, Chemical and Mathematical Sciences for Sustainable Development
Organized by
D.M.S. Mandal's Bhaurao Kakatkar College, Belgaum, Karnataka, India
Website: https://ijmsi.in/
ISSN: 3107-5754 I Vol. 2, Special Issue 1, 2026 I Page No.: 139-151

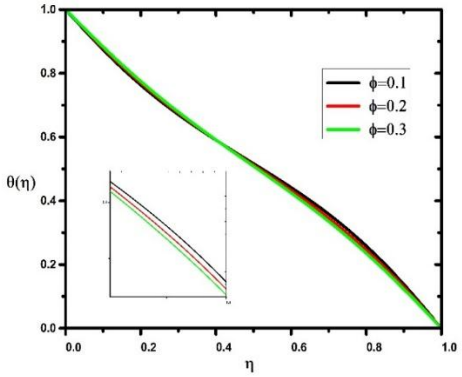

Fig. 8 Temperature profile for different solid volume fraction when $S = -1, M = 0.1$

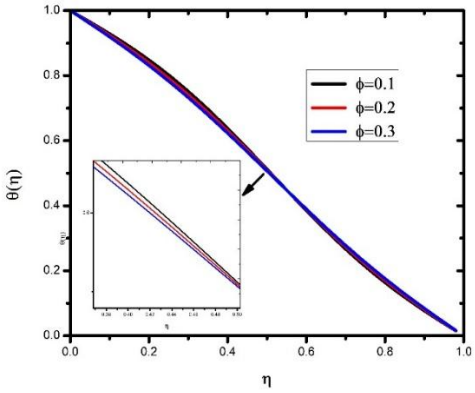

Fig. 9 Temperature profile for different solid volume fraction when $S = 1, M = 0.1$

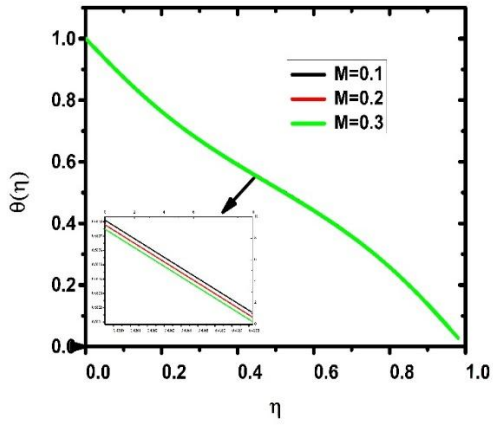

Fig. 10 Temperature profile for different magnetic parameter when $\phi = 0.1, S = -1.$

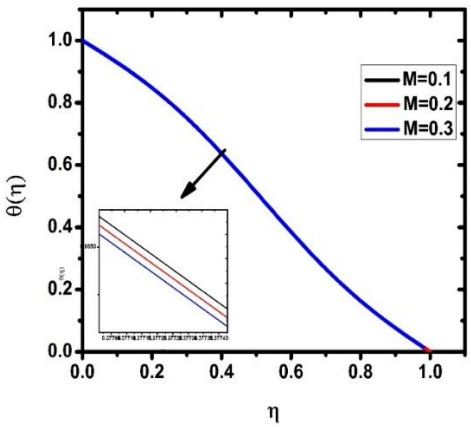

Fig. 11 Temperature profile for different magnetic parameter when $\phi = 0.1, S = 1$

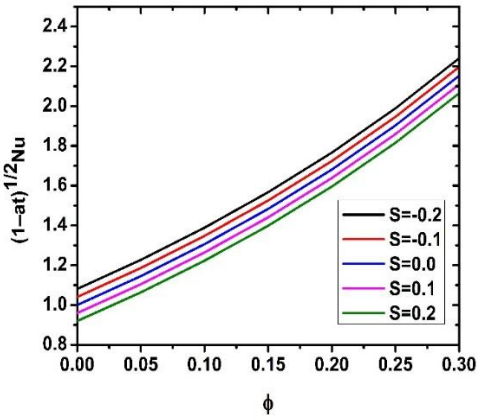

Fig. 12 Nusselt number for different squeeze number when $M = 1$

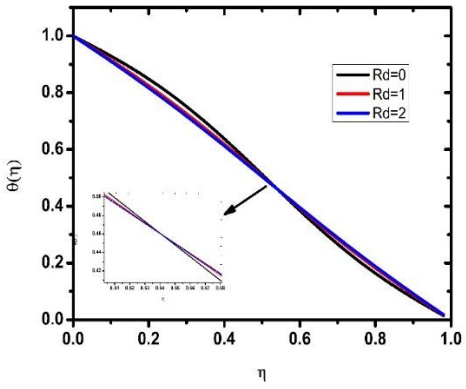

Fig. 12 Nusselt number for different radiation parameter when $M = 0.1, \phi = 0.1, S = 1.$

The thermophysical properties of the base fluid (ethylene glycol) and magnetite nanoparticles are

Website: https://ijmsi.in/
ISSN: 3107-5754 I Vol. 2, Special Issue 1, 2026 I Page No.: 139-151

presented in Table 1. Ethylene glycol possesses relatively low thermal conductivity (0.253) and higher specific heat (2430), whereas magnetite nanoparticles exhibit much higher density (5180) and thermal conductivity (9.7) but lower specific heat (670). Due to this contrast, the addition of nanoparticles significantly enhances the heat transfer capability of the base fluid because of improved thermal conductivity, while at the same time increasing flow resistance owing to higher density and effective viscosity of the nanofluid.

Table 2 shows the comparison of the skin friction coefficient obtained using HPM, FDM, and the Chebyshev pseudo spectral method (CPSM). The results are in excellent agreement, confirming the accuracy and reliability of the CPSM approach. It is observed that the magnitude of skin friction increases with an increase in nanoparticle volume fraction ϕ. This is because the addition of nanoparticles enhances the effective viscosity of the fluid, which increases resistance to flow and consequently raises the wall shear stress. Similarly, an increase in the magnetic parameter (M) also leads to higher skin friction. This behavior is attributed to the Lorentz force generated by the applied magnetic field, which opposes the fluid motion and enhances the shear stress at the wall. Furthermore, the squeeze number (S) exhibits a dual effect: negative values of S reduce the skin friction due to a decelerating or expanding flow that weakens the velocity gradient near the wall, whereas positive values of S increase the skin friction as a result of the squeezing motion that intensifies the velocity gradient.

The influence of various parameters on the velocity profiles is illustrated in Figs. 2–6. It is observed that the velocity increases near the wall as the squeeze number (S) increases from negative to positive values. This is because positive S represents the squeezing of the fluid between the plates, which accelerates the flow and enhances the velocity gradient, whereas negative S corresponds to the separation of the plates, reducing the flow intensity.

The effect of nanoparticle volume fraction ϕ, as shown in Figs. 3 and 4, indicates that the velocity profile decreases with increasing ϕ. This reduction in velocity occurs due to the increase in effective viscosity and density of the nanofluid, which increases internal resistance and suppresses fluid motion. Additionally, Figs. 5 and 6 demonstrate that increasing the magnetic parameter (M) significantly reduces the velocity distribution. This reduction is caused by the Lorentz force induced by the magnetic field, which acts opposite to the flow direction and converts kinetic energy into thermal energy, thereby damping the fluid motion.

The temperature profiles for different parameters are presented in Figs. 7–11. It is observed from Fig. 7 that negative values of the squeeze number (S) lead to a steeper temperature gradient near the wall, indicating enhanced heat transfer, while positive S flattens the temperature profile. This is because decelerating flow increases the residence time of fluid particles near the surface, allowing more heat to be transferred, whereas accelerating flow reduces this interaction time. The influence of nanoparticle volume fraction ϕ, as depicted in Figs. 8 and 9, shows that temperature increases with increasing ϕ. This behavior is due to the enhanced thermal conductivity of the nanofluid, which improves heat diffusion within the fluid. Moreover, Figs. 10 and 11 reveal that increasing the magnetic parameter (M) increases the temperature while reducing the temperature gradient at the wall. This occurs because the magnetic field suppresses fluid motion, weakening convective heat transfer and causing heat to accumulate within the fluid, thereby thickening the thermal boundary layer.

The variation of the Nusselt number is shown in Fig. 12 for different values of the squeeze number (S) and radiation parameter (Rd). It is observed that the Nusselt number increases for negative values of S, indicating enhanced heat transfer due to stronger temperature gradients at the wall in decelerating flows. In contrast, positive S reduces the heat transfer rate. Furthermore, the Nusselt number increases with increasing radiation parameter (Rd). This is because thermal radiation contributes additional energy transport within the fluid, which enhances heat transfer and reduces the thermal boundary layer thickness.

Overall, the results demonstrate a clear trade-off between flow resistance and heat transfer enhancement. The addition of nanoparticles and the

application of a magnetic field improve the thermal performance of the system but at the cost of increased resistance to flow. The squeeze parameter and radiation parameter provide effective control over momentum and heat transfer characteristics. The strong agreement between HPM, FDM, and CPSM validates the Chebyshev pseudo spectral method as a robust and accurate numerical technique for analyzing such nanofluid flow problems.

Conclusion

1. Nanoparticles enhance heat transfer by increasing thermal conductivity, but they also raise skin friction due to higher viscosity.
2. Magnetic fields suppress fluid motion, increasing flow resistance while also affecting the thermal boundary layer.
3. The unsteadiness parameter (S) is a key tuning factor: negative S (decelerating flow) improves heat transfer and reduces friction, whereas positive S has the opposite effect.
4. Thermal radiation (Rd) thins the thermal boundary layer, leading to higher Nusselt numbers and better heat transfer performance.
5. The Chebyshev pseudo-spectral method (CPSM) shows excellent agreement with established methods, confirming its accuracy and reliability for analyzing nanofluid flows.

5. References

1. Choi SUS, Eastman JA. Enhancing thermal conductivity of fluids with nanoparticles. In: ASME International mechanical engineering congress & Exposition. San Francisco, USA ASME; 1995. p. 99–105
2. Choi, S. U. S., 1995. Enhancing thermal conductivity of fluids with nanoparticles. *ASME FED*, 231, pp.99–105.
3. Eastman, J. A., Choi, S. U. S., Li, S., Yu, W. and Thompson, L. J., 2001. Anomalously increased effective thermal conductivities of ethylene glycol-based nanofluids. *Applied Physics Letters*, 78(6), pp.718–720. https://doi.org/10.1063/1.1341218.
4. Xuan, Y. and Li, Q., 2000. Heat transfer enhancement of nanofluids. *International Journal of Heat and Fluid Flow*, 21(1), pp.58–64. https://doi.org/10.1016/S0142-727X(99)00067-3.
5. Das, S. K., Putra, N., Thiesen, P. and Roetzel, W., 2003. Temperature dependence of thermal conductivity enhancement for nanofluids. *Journal of Heat Transfer*, 125(4), pp.567–574. https://doi.org/10.1115/1.1571080.
6. Buongiorno, J., 2006. Convective transport in nanofluids. *Journal of Heat Transfer*, 128(3), pp.240–250. https://doi.org/10.1115/1.2150834.
7. Ishizawa, S., 1966. The unsteady flow between parallel disks. *Bulletin of JSME*, 9, pp.533–550. https://doi.org/10.1299/jsme1958.9.533
8. Mellor, G. L., Chapple, P. J. and Stokes, A. N., 1968. Flow between rotating disks. *Journal of Fluid Mechanics*, 31, pp.95–112. https://doi.org/10.1017/S0022112068000134.
9. Nazir, U. and Mahmood, T., 2010. Heat transfer analysis between rotating disks. *Applied Mathematical Modelling*, 34, pp.274–289. https://doi.org/10.1016/j.apm.2009.03.016.
10. Hayat, T., Ahmad, M. W., Qayyum, S. and Alsaedi, A., 2020. Irreversibility analysis in squeezing nanofluid flow with thermal radiation. *Multidiscipline Modeling in Materials and Structures*. https://doi.org/10.1108/MMMS-01-2020-0015.
11. Zainal, N., Nazar, R., Naganthran, K. and Pop, I., 2021. MHD and thermal radiation effects on hybrid nanofluid flow. *International Journal of Heat and Fluid Flow*. https://doi.org/10.1016/j.ijheatfluidflow.2020.108785.

12. Hosseinzadeh, K., Mogharrebi, A.R., Asadi, A., Sheikhshahrokhdehkordi, M., Mousavisani, S. and Ganji, D.D., 2022. Entropy generation analysis of mixture nanofluid (H2O/c2H6O2)–Fe3O4 flow between two stretching rotating disks under the effect of MHD and nonlinear thermal radiation. *International Journal of Ambient Energy*, *43*(1), pp.1045-1057. https://doi.org/10.1080/01430750.2019.1681294
13. Awati, V. B., Goravar, A. and Kumar, M. N., 2023. Spectral and Haar wavelet collocation method for the solution of heat generation and viscous dissipation in micro-polar nanofluid for MHD stagnation point flow. *Mathematics and Computers in Simulation*, 212, pp.173–191. https://doi.org/10.1016/j.matcom.2023.07.031.
14. Awati, V. B., Goravar, A., Kumar, M. N. and Bognár, G., 2023. Stability analysis of magnetohydrodynamic Casson fluid flow and heat transfer past an exponentially shrinking surface by spectral approach. *Results in Physics*, 49, p.106511. https://doi.org/10.1016/j.rinp.2023.106511.
15. El Harfouf, A., Wakif, A. and Mounir, S. H., 2024. MHD squeezing flows of reacting-radiating Maxwell nanofluids. *Journal of Umm Al-Qura University for Applied Sciences*. https://doi.org/10.1007/s43994-024-00139-9
16. Al Sankoor, A. B., et al., 2024. Thermal and flow dynamics of MHD hybrid nanofluids considering radiation effects. *International Journal of Heat and Fluid Flow*. https://doi.org/10.1016/j.csite.2024.105229
17. Irreversibility and sensitivity analysis of MHD squeezing nanofluid flow between parallel permeable disks, 2025. *International Journal of Thermofluids*. https://doi.org/10.1016/j.ijft.2025.101109
18. Vigneshwari, S., Reddappa, B., Sumithra, A. et al., 2025. Thermal and flow dynamics of unsteady MHD nanofluid convection with porous medium. *Journal of Thermal Analysis and Calorimetry*. https://doi.org/10.1007/s10973-025-14025-x
19. Johari, M., Hoshyar, H. A., Dabirian, E. et al., 2025. Advanced thermal management in MHD nanofluid systems with Cattaneo-Christov heat flux. *Scientific Reports*. https://doi.org/10.1038/s41598-025-04011-6
20. Motsa, S. S., Shateyi, S. and Makukula, Z. G., 2014. A new spectral relaxation method for nonlinear boundary layer flow problems. *Journal of Applied Mathematics*, 2014, p.423628. https://doi.org/10.1155/2014/423628.
21. Farcy, A. and de Roquefort, T., 1988. Chebyshev pseudospectral solution of the incompressible Navier–Stokes equations in curvilinear domains. *Computers & Fluids*, 16(4), pp.459–473. https://doi.org/10.1016/0045-7930(88)90030-0.
22. Guo, B. Y. and Li, J., 1994. Fourier-Chebyshev pseudospectral method for two-dimensional vorticity equation. *Numerische Mathematik*, 66(3), pp.329–346. https://doi.org/10.1007/BF01385653.
23. Elazem, N. Y. and Ebaid, A., 2016. Numerical analysis via Chebyshev pseudospectral method for nonlinear initial/boundary value problems. *Journal of Mathematics and Computer Science*, 6(4), pp.597–619. https://doi.org/10.22436/jmcs.06.04.10 is this correct`
24. Elgazery, N. S., 2008. An implicit-Chebyshev pseudospectral method for the effect of radiation on power-law

fluid past a vertical plate immersed in a porous medium. *Communications in Nonlinear Science and Numerical Simulation*, 13, pp.728–744. https://doi.org/10.1016/j.cnsns.2006.12.013.

25. Oloniiju, S. D., Mukwevho, N. and Tijani, Y. O., 2024. Chebyshev pseudospectral method for fractional differential equations. *AppliedMath*, 4(3), pp.950–974. https://doi.org/10.3390/appliedmath4030051

26. Sampath Kumar, V. S., Devaki, B., Bhat, P. G., Pai, N. P., Vasanth, K. R. and Ganesh Kumar, K., 2024. Analysis of flow and heat transfer characteristics of ethylene glycol-based magnetite nanoparticles squeezed between parallel disks with magnetic effect. *Journal of Thermal Analysis and Calorimetry*, 149, pp.12219–12230. https://doi.org/10.1007/s10973-024-13481-1.

27. Elnagar, G., Kazemi, M. A. and Razzaghi, M., 1995. The pseudospectral Legendre method for discretizing optimal control problems. *IEEE Transactions on Automatic Control*, 40(10), pp.1793–1796. https://doi.org/10.1109/9.467672.

28. Fahroo, F. and Ross, I. M., 2002. Direct trajectory optimization by a Chebyshev pseudospectral method. *Journal of Guidance, Control, and Dynamics*, 25(1), pp.160–166. https://doi.org/10.2514/2.4852.

29. Yousefian, A., Sahoo, A. and Narayanan, V., 2024. A novel online pseudospectral method for approximation of nonlinear systems dynamics. *Nonlinear Dynamics*, 115(2), pp.1235–1254. https://doi.org/10.1007/s11071-023-088.

*****